AIAA JOURNAL
Vol. 36, No. 8, August 1998

Elasticity Approach for Delamination Buckling of Composite Beam Plates

Haozhong Gu* and Aditi Chattopadhyay†
Arizona State University, Tempe, Arizona 85287-6106

An elasticity-theory-based approach is developed for delamination buckling of simply supported composite laminates whose behavior is referred to as cylindrical bending. The approach ensures an accurate description of the transverse shear and the transverse normal effects in delamination buckling of composite plates. The uniform prebuckling stress assumption, which is comparable to the membrane assumption used in plate theories, is made for deriving the elasticity-theory-based buckling equations. The closed-form expressions for the displacements and stresses are derived, and the nonlinear eigenvalue equations that are used to solve for critical loads are presented. The results obtained from the elasticity solution are compared with the critical loads furnished by the existing classical laminate theory and a previously developed higher-order shear deformation theory. The solution provides a means of accurate assessment of existing plate theories used in delamination buckling problems.

I. Introduction

DELAMINATION buckling of anisotropic plates and laminated composite plates is usually analyzed by using approximate laminated plate theories based on either the classical Kirchhoff–Love hypothesis of nondeformable normals and transverse shears[1−5] or the refined displacement field accounting for the effects of transverse shear deformation or normal stress.[6−9] The major limitation of these laminated plate theories in the description of laminate response is the approximation of in-plane displacements through the thickness, particularly for laminates in which the stiffness properties vary dramatically from layer to layer. Other important limiting factors are the presence of boundary conditions in the plate theories that precludes the precise calculation of boundary-layer effects implied by the hypothesis of plate theories. Finally, the assumption of a state of plane stress in the constitutive relations eliminates the possibility of rigorous calculation of interlaminar stresses.

To assess the validity of these approximate theories, rigorous analytical solutions based on the exact theory of elasticity should be obtained for plate problems that are amenable to such analysis. Such benchmark elasticity solutions are valuable for laminated composite plates with inherent anisotropy in material and inherent inhomogeneity among the different layers. The anisotropy and inhomogeneity lead to considerable warping of the normal to the middle surface of the plate and cause abrupt variations of stresses at the interfaces of the laminate.

A number of elasticity solutions are available for composite plates without delamination subjected to a transverse load distribution. Pagano[10] first analyzed the cylindrical bending of a simply supported composite laminate under sinusoidal transverse loads. Later investigations include bending of finite rectangular plates,[11,12] off-axial layers,[13,14] and localized loading.[15] These elasticity solutions have enabled us to quantify the errors associated with various laminated plate theories. Recently Chattopadhyay and Gu[16] obtained the exact elasticity solution to characterize delamination buckling of orthotropic plates and composite laminates without delamination. However, no research has been reported to date for solving delamination problems in composites by using the elasticity approach. This is obviously due to the greater complexity of the governing equations.

Toward this objective, an elasticity solution is presented for delamination buckling of simply supported orthotropic plates and laminated composite plates whose behavior is referred to as cylindrical bending in this paper. Results are presented for anisotropic laminates with various stacking sequences. The influence of delamination lengths and locations on the critical buckling load is also studied. Finally, the accuracy of the classical lamination theory[3] and a previously developed higher-order shear deformation theory,[16] for delamination buckling, is studied by comparing their results with those obtained using the elasticity-based approach. The developed approach therefore serves as a tool to assess the accuracy of the existing approaches. Comparisons are made for composites with moderately thick and thick constructions. The cylindrical bending behavior and the uniform prebuckling stress assumption implies that the current model can be properly used in the cases with symmetric and cross-ply composites.

II. Formulation

A. Buckling Equation

To derive the elasticity-theory-based buckling equations, the nonlinear strain-displacement relation needs to be considered. The two-dimensional nonlinear strain-displacement relation can be expressed as

$$\varepsilon_{\alpha\beta} = \tfrac{1}{2}(u_{\alpha,\beta} + u_{\beta,\alpha} + u_{\gamma,\alpha}u_{\gamma,\beta}), \qquad \alpha,\ \beta,\ \gamma = 1, 2 \tag{1}$$

where $\varepsilon_{\alpha\beta}$ are the strain components, u_γ are the displacements, and a comma denotes partial differentiation with respect to the index that follows. A set of equilibrium equations and associated boundary conditions can also be derived using a variational principle:

$$\begin{aligned}\delta\Pi &= \int_A \sigma_{\alpha\beta}\delta\varepsilon_{\alpha\beta}\,\mathrm{d}A - \int_S p_\gamma \delta u_\gamma\,\mathrm{d}S = \int_A \sigma_{\alpha\beta}(\delta u_{\alpha,\beta} + u_{\gamma,\alpha}\delta u_{\gamma,\beta})\,\mathrm{d}A \\ &\quad - \int_S p_\gamma\delta u_\gamma\,\mathrm{d}S = \int_A [\sigma_{\alpha\beta}(\delta_{\gamma\alpha} + u_{\gamma,\alpha})]_{,\beta}\delta u_\gamma\,\mathrm{d}A \\ &\quad - \int_S [\sigma_{\alpha\beta}(\delta_{\gamma\alpha} + u_{\gamma,\alpha})n_\beta - p_\gamma]\delta u_\gamma\,\mathrm{d}S\end{aligned} \tag{2}$$

where A and S denote the area and the boundary of the two-dimensional elastic body, respectively. Quantities $\sigma_{\alpha\beta}$ are the stress components, and n_β is the normal vector at the boundary. This leads to the following equilibrium equations:

$$[\sigma_{\alpha\beta}(\delta_{\gamma\alpha} + u_{\gamma,\alpha})]_{,\beta} = 0 \tag{3}$$

and the associated boundary conditions

$$\sigma_{\alpha\beta}(\delta_{\gamma\alpha} + u_{\gamma,\alpha})n_\beta = p_\gamma \qquad \text{or} \qquad u_\gamma = 0 \tag{4}$$

Presented as Paper 96-1612 at the AIAA/ASME/ASCE/AHS/ASC 37th Structures, Structural Dynamics, and Materials Conference, Salt Lake City, UT, April 15–17, 1996; received Sept. 13, 1996; revision received March 20, 1998; accepted for publication April 27, 1998.

*Postdoctoral Fellow, Department of Mechanical and Aerospace Engineering. Member AIAA.

†Professor, Department of Mechanical and Aerospace Engineering. Associate Fellow AIAA.

At the critical load, there are two possible infinitely close positions of equilibrium. Using a superscript 0 to denote the components of the stresses or the displacements corresponding to the primary position, a perturbed position is defined as follows:

$$\sigma_{\alpha\beta} = \sigma^0_{\alpha\beta} + \alpha\sigma^1_{\alpha\beta}, \qquad u_\gamma = u^0_\gamma + \alpha u^1_\gamma \tag{5}$$

where α is an infinitesimally small quantity and $\alpha(\,)^1$ are the stresses or the displacements necessary to shift from the initial position of equilibrium to the new equilibrium position. Substituting Eq. (5) into Eq. (4) and linearizing the obtained equations, one can derive the buckling equations and the associated boundary conditions

$$\left[\sigma_{\alpha\beta}\left(\delta_{\gamma\alpha} + u^0_{\gamma,\alpha}\right) + \sigma^0_{\alpha\beta}u_{\gamma,\alpha}\right]_{,\beta} = 0 \tag{6}$$

$$\left[\sigma_{\alpha\beta}\left(\delta_{\gamma\alpha} + u^0_{\gamma,\alpha}\right) + \sigma^0_{\alpha\beta}u_{\gamma,\alpha}\right]n_\beta = 0 \qquad \text{or} \qquad u_\gamma = 0 \tag{7}$$

where the superscripts 1 are removed for simplification. The equilibrium equations and boundary conditions for a prebuckling state are as follows:

$$\sigma^0_{\alpha\beta,\beta} = 0 \tag{8}$$

$$\sigma^0_{\alpha\beta}n_\beta = p_\alpha \qquad \text{or} \qquad u^0_\gamma = 0 \tag{9}$$

For composite plates subjected to in-plane load with the coordinate system described in Fig. 1, the preceding prebuckling equilibrium equations and the associated boundary conditions can be rewritten in the following form:

$$\sigma^0_{x,x} + \tau^0_{xz,z} = 0, \qquad \tau^0_{xz,x} + \sigma^0_{z,z} = 0 \tag{10}$$

$$\begin{aligned} \sigma^0_x = -p, \qquad \tau^0_{xz} = 0 \qquad &\text{at} \qquad x = L/2,\ L/2 \\ \sigma^0_z = \tau^0_{xz} = 0 \qquad &\text{at} \qquad z = -h/2,\ h/2 \end{aligned} \tag{11}$$

or

$$u^0 = w^0 = 0$$

For single-layered orthotropic plates and composite plates with unidirectional layers, the prebuckling stress can be solved from Eqs. (10) and (11) exactly:

$$\sigma^0_x = -p, \qquad \sigma^0_z = \tau^0_{xz} = 0 \tag{12}$$

For multilayered composite plates with different orientations, Eqs. (10) are valid in each individual layer. However, the stress boundary conditions $\sigma^0_z = \tau^0_{xz} = 0$ are true only at plate surfaces. Prebuckling stresses σ^0_z and τ^0_{xz} are no longer zero at the layer interfaces. This results in a very complicated set of equations governing the prebuckling state. Also it leads to unsolvable buckling equations. Therefore, the assumption of the uniform prebuckling stress state is made in this paper, which enforces the solution in Eqs. (12) to be valid for prebuckling states in multilayered composite plates. This assumption is comparable to the membrane prebuckling state assumed in plate theories. Next, by employing the exact constitutive equations for any orthotropic layer whose material axes are parallel to the geometric axes,

$$\begin{bmatrix} \sigma_x \\ \sigma_z \\ \tau_{xz} \end{bmatrix} = \begin{bmatrix} C'_{11} & C'_{13} & 0 \\ C'_{13} & C'_{33} & 0 \\ 0 & 0 & C'_{55} \end{bmatrix} \begin{bmatrix} u_{,x} \\ w_{,z} \\ u_{,z} + w_{,x} \end{bmatrix} \tag{13}$$

the displacements for the prebuckling state are derived as follows:

$$\begin{gathered} u^0_{,x} = -\frac{C'_{33}}{C'_{11}C'_{33} - C'^2_{13}}p, \qquad w^0_{,z} = -\frac{C'_{13}}{C'_{11}C'_{33} - C'^2_{13}}p \\ u^0_{,z} = w^0_{,x} = 0 \end{gathered} \tag{14}$$

in which the reduced stiffness coefficients for plane strain C'_{ij} $(i,\ j = 1,\ 3)$ can be derived from the general three-dimensional constitutive equations in terms of C_{ij}. The prebuckling state of the two-dimensional elastic body is therefore determined.

Introducing constitutive equations [Eqs. (13)] into the buckling equations [Eqs. (6)] and using determined prebuckling stresses and displacements [Eqs. (12) and (14)], one obtains the buckling equations in terms of displacements:

$$\begin{aligned} &\left(1 - \frac{C'_{33}}{C'_{11}C'_{33} - C'^2_{13}}p\right)[C'_{11}u_{,xx} + C'_{55}u_{,zz} + (C'_{13} + C'_{55})w_{,xz}] \\ &\quad - pu_{,xx} = 0 \\ &\left(1 + \frac{C'_{13}}{C'_{11}C'_{33} - C'^2_{13}}p\right)[(C'_{13} + C'_{55})u_{,xz} + C'_{55}w_{,xx} + C'_{33}w_{,zz}] \\ &\quad - pw_{,xx} = 0 \end{aligned} \tag{15}$$

or

$$w_{,zzzz} - aw_{,xxzz} + bw_{,xxxx} = 0 \tag{16a}$$

with

$$\begin{aligned} a = \frac{1}{C'_{33}C'_{55}}\Bigg[&C'_{11}C'_{33} - C'^2_{13} - 2C'_{13} + C'_{55} \\ &- \frac{C'_{33}p}{1 - C'_{33}p/\left(C'_{11}C'_{33} - C'^2_{13}\right)} - \frac{C'_{55}p}{1 + C'_{13}p/\left(C'_{11}C'_{33} - C'^2_{13}\right)}\Bigg] \end{aligned}$$

$$\begin{aligned} b = \frac{1}{C'_{33}C'_{55}}&\left[C'_{11} - \frac{p}{1 - C'_{33}p/\left(C'_{11}C'_{33} - C'^2_{13}\right)}\right] \\ &\times \left[C'_{55} - \frac{p}{1 + C'_{13}p/\left(C'_{11}C'_{33} - C'^2_{13}\right)}\right] \end{aligned} \tag{16b}$$

Equations (16) are the buckling equations used in this paper. The associated boundary conditions described in Eqs. (7) can also be rewritten in the following form:

$$\begin{aligned} \sigma_x\left(1 + u^0_{,x}\right) - pu_{,x} = 0, \qquad \tau_{xz}\left(1 + w^0_{,z}\right) - pw_{,x} = 0 \qquad &\text{at} \qquad x = -L/2,\ L/2 \\ \tau_{xz} = 0, \qquad \sigma_z = 0 \qquad &\text{at} \qquad z = -h/2,\ h/2 \end{aligned} \tag{17a}$$

or

$$u = w = 0$$

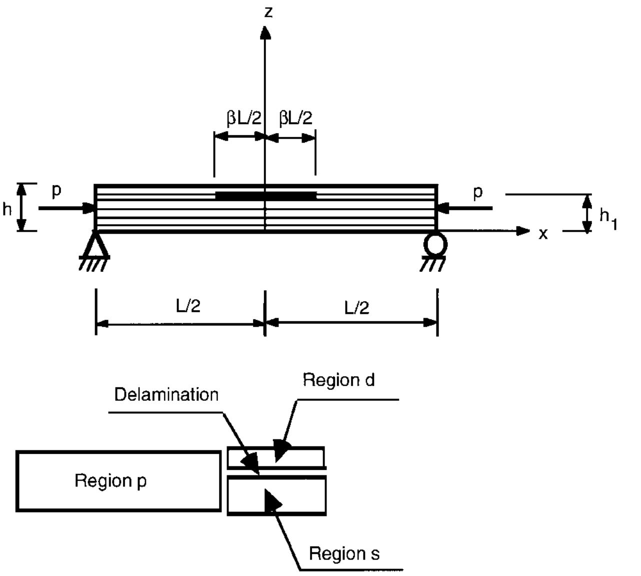

Fig. 1 Geometry of the composites with delamination.

or in terms of displacements

$$\left[C'_{11} - \frac{p}{1 - C'_{33}p/\left(C'_{11}C'_{33} - C'^2_{13}\right)}\right]u_{,x} + C'_{13}w_{,z} = 0$$

$$C'_{55}u_{,z} + \left[C'_{55} - \frac{p}{1 - C'_{33}p/\left(C'_{11}C'_{33} - C'^2_{13}\right)}\right]w_{,x} = 0 \tag{17b}$$

$$\text{at} \qquad x = -\frac{L}{2}, \frac{L}{2}$$

$$u_{,z} + w_{,x} = 0, \qquad C'_{13}u_{,x} + C'_{33}w_{,z} = 0 \qquad \text{at} \qquad z = -\frac{h}{2}, \frac{h}{2}$$

or

$$u = w = 0$$

B. Assumed Solution

For composite laminates with delamination, it is assumed that the delamination separates the laminate across length and thickness into three regions (see Fig. 1), the perfect region or undelaminated region (region p), the delaminated layer (region d), and the sublaminate (region s). Therefore, in each one of these regions the elasticity approach derived for plates without delamination is applicable. A key issue associated with the delamination buckling problem is the solution formulation in each region. For simply supported plates in the region without delamination (p), the boundary conditions for the buckling state are given by

$$\left[C'_{11} - \frac{p}{1 - C'_{33}p/\left(C'_{11}C'_{33} - C'^2_{13}\right)}\right]u_{,x} + C'_{13}w_{,z} = 0$$

$$\text{at} \qquad x = -\frac{L}{2}, \frac{L}{2} \tag{18}$$

$$w = 0$$

where L is the length of the plate. Therefore the assumed solution form for the deflection in the region without delamination, w_p, is written as

$$w_p = f_p(z)\cos q_p x, \qquad \beta L/2 \le |x| \le L/2 \tag{19}$$

where $f_p(z)$ is an unknown function of z and the quantity q_p is defined as follows:

$$q_p = q_p(n) = n\pi/L \tag{20}$$

Note that for the beam plate the lowest critical buckling load is always accompanied by a single half-buckling wave, $n = 1$. Solution forms for the deflections in the delamination regions for delaminated layer (d), w_d, and sublaminate (s), w_s, are assumed to be effectively expressed by two terms that represent the solutions of the buckling problem for the Euler–Bernouli beam in a symmetric case:

$$\begin{aligned} w_d &= f_d(z)\cos q_d x + B_d, \qquad h_1 \le z \le h/2 \\ w_s &= f_s(z)\cos q_s x + B_s, \qquad -h/2 \le z \le h_1 \end{aligned} \qquad |x| \le L/2 \tag{21}$$

where B_d and B_s are unknown constants, $f_d(z)$ and $f_s(z)$ are unknown functions of z describing the behavior of the delaminated layer and the sublaminate, and the quantities q_d and q_s are defined as

$$q_d = q_d(k_d) = k_d\pi/\beta L, \qquad q_s = q_s(k_s) = k_s\pi/\beta L \tag{22}$$

where k_d and k_s are unknown constants. The buckling equation, which is satisfied by these assumed solutions, can be written as

$$f_t^{(4)}(z) - 2a_t(C'_{ij}, p)q_t^2 f_t''(z) + b_t(C'_{ij}, p)q_t^4 f_t(z) = 0$$

$$t = p, d, s \tag{23a}$$

where the forms of parameters a_t and b_t are expressed as

$$a_t = \frac{1}{2C'_{33}C'_{55}}\left[C'_{11}C'_{33} - C'^2_{13} - 2C'_{13} + C'_{55} - \frac{C'_{33}p}{1 - C'_{33}p/\left(C'_{11}C'_{33} - C'^2_{13}\right)} - \frac{C'_{55}p}{1 + C'_{13}p/\left(C'_{11}C'_{33} - C'^2_{13}\right)}\right] \tag{23b}$$

$$b_t = \frac{1}{C'_{33}C'_{55}}\left[C'_{11} - \frac{p}{1 - C'_{33}p/\left(C'_{11}C'_{33} - C'^2_{13}\right)}\right] \times \left[C'_{55} - \frac{p}{1 + C'_{13}p/\left(C'_{11}C'_{33} - C'^2_{13}\right)}\right]$$

The solutions of the unknown functions $f_t(z)$ are written as

$$f_t(z) = \sum_{j=1}^{4} A_j^t \exp\left(m_j^t z\right), \qquad t = p, d, s \tag{24}$$

where A_j^t are constants, provided that m_j^t are all distinct. The various values m_j^t are given by

$$\begin{matrix} m_1^t \\ m_2^t \end{matrix} = \pm q_t\sqrt{a_t + \sqrt{a_t^2 - b_t}}, \qquad \begin{matrix} m_3^t \\ m_4^t \end{matrix} = \pm q_t\sqrt{a_t - \sqrt{a_t^2 - b_t}} \tag{25}$$

The solutions for the in-plane displacement u_t ($t = d, s$) in the delamination regions, for the delaminated layer and the sublaminate, can be obtained as follows:

$$u_t = g_t(z)\sin q_t x + D_t x, \qquad t = p, d, s \tag{26}$$

where D_t is the unknown constant and $g_t(z)$ is a function of z that describes the behavior of the delaminated layer and the sublaminate,

$$g_t(z) = \sum_{j=1}^{4} E_j^t \exp\left(m_j^t z\right), \qquad t = p, d, s \tag{27}$$

where E_j^t are constants that can be expressed by A_j^t and C'_{ij}, and the quantities m_j^t are described in Eq. (25). The displacement and stress components now take the form

$$w_t = \cos q_t x \sum_{j=1}^{4} A_j^t \exp\left(m_j^t z\right) + B_t$$

$$u_t = \frac{1}{(C'_{13} + C'_{55})}\left(\sum_{j=1}^{4}\left\{C'_{33}m_j^t - \left[C'_{55} - \frac{p}{1 + C'_{13}p/\left(C'_{11}C'_{33} - C'^2_{13}\right)}\right]\frac{q_t}{m_j^t}\right\} \times A_j^t \exp\left(m_j^t z\right)\right)\sin q_t x + D_t x, \qquad t = p, d, s$$

$$\sigma_x^t = \left[\sum_{j=1}^{4}\left(C'_{13}m_j^t + \frac{C'_{11}q_t}{C'_{13} + C'_{55}}\left\{C'_{33}m_j^t - \left[C'_{55} - \frac{p}{1 + C'_{13}p/\left(C'_{11}C'_{33} - C'^2_{13}\right)}\right]\frac{q_t}{m_j^t}\right\}\right) \times A_j^t \exp\left(m_j^t z\right)\right]\cos q_t x + C'_{11}D_t$$

$$\sigma_z^t = \left[\sum_{j=1}^{4}\left(C'_{33}m_j^t + \frac{C'_{13}q_t}{C'_{13} + C'_{55}}\left\{C'_{33}m_j^t - \left[C'_{55} - \frac{p}{1 + C'_{13}p/\left(C'_{11}C'_{33} - C'^2_{13}\right)}\right]\frac{q_t}{m_j^t}\right\}\right) \times A_j^t \exp\left(m_j^t z\right)\right]\cos q_t x + C'_{13}D_t$$

$$\tau^t_{xz} = C'_{55}\left[\sum_{j=1}^{4}\left(\frac{1}{C'_{13}+C'_{55}}\left\{C'_{33}m^{t^2}_j - \left[C'_{55} - \frac{p}{1+C'_{13}p/\left(C'_{11}C'_{33}-C'^2_{13}\right)}\right]q_t\right\} - q_t\right) \times A^t_j \exp\left(m^t_j z\right)\right]\sin q_t x \tag{28}$$

It must be noted that the solutions in Eqs. (28) satisfy the boundary condition written in Eqs. (18). The remaining stress-free boundary conditions at the top and the bottom surfaces and the delamination interface, for the buckling state, are described by Eqs. (17):

$$\begin{aligned} &\sigma_z(x,0) = \tau_{xz}(x,0) = 0 \\ &\sigma_z(x,h) = \tau_{xz}(x,h) = 0 \end{aligned} \qquad -L/2 \le x \le L/2$$

$$\begin{aligned} &\sigma_z(x,h_1^-) = \tau_{xz}(x,h_1^-) = 0 \\ &\sigma_z(x,h_1^+) = \tau_{xz}(x,h_1^+) = 0 \end{aligned} \qquad -\beta L/2 \le x \le \beta L/2 \tag{29}$$

where h is the plate thickness; h_1 denotes the delamination position along the z direction (see Fig. 1), and the superscripts $+$ and $-$ indicate quantities related to the buckling layer and sublaminate layer, respectively.

C. Continuity Equation

Because the continuity of displacements between the region with delamination and the region without delamination cannot be matched exactly, it is now assumed that these conditions are satisfied in an average sense as follows:

$$\begin{aligned} \int_0^{h_1} u_s|_{x=\beta L/2}\,\mathrm{d}z &= \int_0^{h_1} u_p|_{x=\beta L/2}\,\mathrm{d}z \\ \int_0^{h_1} w_s|_{x=\beta L/2}\,\mathrm{d}z &= \int_0^{h_1} w_p|_{x=\beta L/2}\,\mathrm{d}z \\ \int_{h_1}^{h} u_d|_{x=\beta L/2}\,\mathrm{d}z &= \int_{h_1}^{h} u_p|_{x=\beta L/2}\,\mathrm{d}z \\ \int_{h_1}^{h} w_d|_{x=\beta L/2}\,\mathrm{d}z &= \int_{h_1}^{h} w_p|_{x=\beta L/2}\,\mathrm{d}z \end{aligned} \tag{30}$$

where h_1 is the position of the delamination in the z direction (see Fig. 1).

To establish continuity of traction and displacement at the interfaces between layers, excluding the delamination interface where $(-\beta L/2 \le x \le \beta L/2, z = h_1)$, the following conditions must be satisfied in local coordinates:

$$\begin{aligned} &\tau^{(i)}_{xz}(x,h_i) = \tau^{(i+1)}_{xz}(x,0), && \sigma^{(i)}_z(x,h_i) = \sigma^{(i+1)}_z(x,0) \\ &u^{(i)}(x,h_i) = u^{(i+1)}(x,0), && w^{(i)}(x,h_i) = w^{(i+1)}(x,0) \end{aligned}$$
$$i = 1,2,\ldots,m-1 \tag{31}$$

where the quantity h_i denotes the thickness of the ith layer ($i = 1, 2, \ldots, m$, where m is the number of layers) and

$$h = \sum_{i=1}^{m} h_i$$

is the total plate thickness. The superscript i is used to identify quantities in the ith layer.

If the unknown constants k_d and k_s are provided, Eqs. (19–21) constitute a nonlinear eigenvalue problem for algebraic equations, with p as the parameter. The general form of this nonlinear eigenvalue problem is expressed as

$$\boldsymbol{A}(p)\boldsymbol{a} = 0 \tag{32}$$

where vector $\boldsymbol{a}$ consists of the undetermined constants A^t_j, B_t, and D_t. Using the Taylor series expansion, one can write Eq. (22) as follows:

$$\left(\boldsymbol{A}_0 - p\boldsymbol{A}_1 - p^2\boldsymbol{A}_2 - \cdots - p^k\boldsymbol{A}_k - \cdots\right)\boldsymbol{a} = 0 \tag{33}$$

To solve for the constants k_d and k_s, the continuity of rotations between the region with delamination and the region without delamination is required. The conditions are also satisfied in the average sense. According to the theory of elasticity, the continuity of rotations can be written as

$$\begin{aligned} \int_0^{h_1}\left(\frac{\partial u_s}{\partial z} - \frac{\partial w_s}{\partial x}\right)_{x=\beta L/2}\mathrm{d}z &= \int_0^{h_1}\left(\frac{\partial u_p}{\partial z} - \frac{\partial w_p}{\partial x}\right)_{x=\beta L/2}\mathrm{d}z \\ \int_{h_1}^{h}\left(\frac{\partial u_d}{\partial z} - \frac{\partial w_d}{\partial x}\right)_{x=\beta L/2}\mathrm{d}z &= \int_{h_1}^{h}\left(\frac{\partial u_p}{\partial z} - \frac{\partial w_p}{\partial x}\right)_{x=\beta L/2}\mathrm{d}z \end{aligned} \tag{34}$$

D. Iterative Procedure

An iterative method is employed to solve the delamination buckling problem as follows.

1) Set initial values of k_{d0} and k_{s0}.

2) Solve the eigenvalue problem for $(p, \boldsymbol{a})$ using Eq. (33). The symbolic manipulation software Mathematica is used to derive the symbolic form of $\det \boldsymbol{A} = 0$ with respect to eigenvalue (critical load) p. Solve for p and the eigenvector $\boldsymbol{a}$.

3) Use the continuity equation of rotation described in Eq. (34) to obtain Δk_{di} and Δk_{si}.

4) Check criterion for convergence ($\Delta k_{di}/k_{di} \le 10^{-N}$, $\Delta k_{si}/k_{si} \le 10^{-N}$, where N is an integer). If they are not satisfied, go to step 5; if they are satisfied, stop the iteration procedures and solutions are obtained.

5) Use equations $k_{d(i+1)} = k_{di} + \Delta k_{di}$ and $k_{s(i+1)} = k_{si} + \Delta k_{si}$ to obtain new values to start another iteration (go to step 2).

It must be noted that once the good initial values k_{d0} and k_{s0} are provided, which are close to the value of 2 (implying they are close to clamped boundary conditions), the iteration procedure normally converges.

III. Results and Discussion

As an illustrative example, the critical load was determined for a delaminated unidirectional composite plate with various delamination lengths. The material properties (typical for graphite/epoxy composites) are listed next, where L signifies the direction parallel to the fibers, T is the transverse direction, and ν_{LT} is the Poisson ratio measuring strain in the transverse direction under uniaxial normal stress in the L direction: $E_L = 25 \times 10^6$ psi, $E_T = 10^6$ psi, $G_{LT} = 0.5 \times 10^6$ psi, $G_{TT} = 0.2 \times 10^6$ psi, and $\nu_{LT} = \nu_{TT} = 0.25$.

Here the quantity h_1/h (see Fig. 1) represents the location of the delamination along the thickness. A larger value of this ratio indicates a near-surface delamination. The ratio also indicates the relative thickness of the delaminated layer, defined in region d in Fig. 1, to the plate thickness. The larger the ratio, the thinner the delaminated layer. Therefore, the case with a large ratio of h_1/h will be referred to as the thin delamination case and the case with a small ratio will be referred to as the thick delamination case. The plate in this example is thick $L/h = 10$, and the delaminated layer is relatively thin ($h_1/h = 0.9$).

Figure 2 presents the critical loads, which are normalized with respect to the value calculated by the classical laminate theory (CLT).

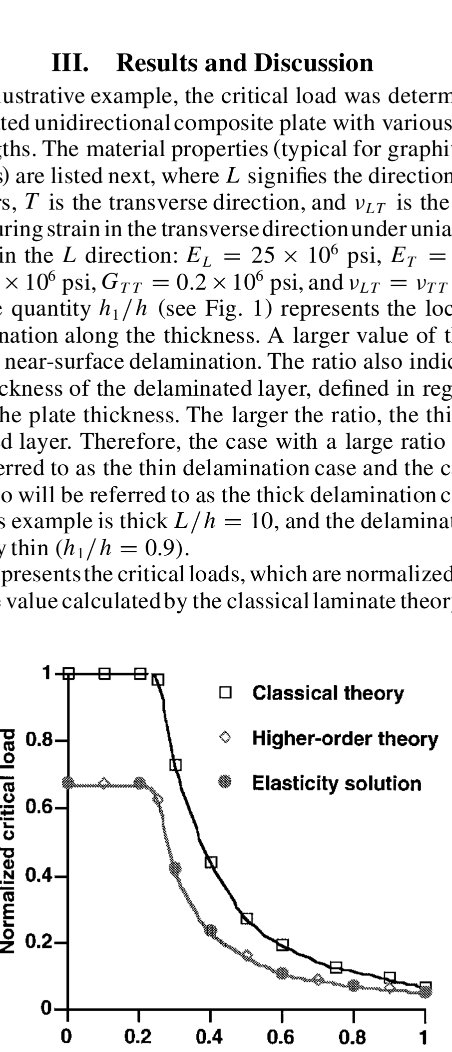

Fig. 2 Variation of critical load with delamination length β for unidirectional composites; $h_1/h = 0.9$ and $L/h = 10$.

Comparisons are made between the solution obtained from the elasticity theory and those obtained using the classical laminate theory[3] and the higher-order theory[6] for a wide range of delamination length β. It is seen, from Fig. 2, that although the CLT exhibits a significant deviation, the results of the new higher-order theory show good agreement with those using the elasticity solution over the entire range of the delamination length. Because the higher-order theory does not account for the transverse normal effect, this agreement indicates that the transverse normal effect is negligible in the delamination buckling problem of simply supported unidirectional plates. This agrees with the observation made by the authors in addressing buckling of composite plates without delamination.[16] Moreover, the numbers of the half-buckling wave in delaminated regions, k_d and k_s, are varied over the entire range of the delamination length. With long delamination length, they are close to 2. For example, in the case of $\beta = 0.8$, the values are $k_d = 1.985$ and $k_s = 1.992$. This indicates that the delaminated layer and the sublaminate deflect in different ways and their conditions at the region interfaces are close to clamped boundary conditions. Therefore, the delamination buckling in this case is governed by a local buckling mode. With short delamination length, they are a little bit away from 2. In the case of $\beta = 0.2$, the values are $k_d = 1.927$ and $k_s = 1.926$. The very close values of k_d and k_s indicate that the delaminated layer and the sublaminate deflect together in the delaminated region where they are governed by the global buckling mode. The curves of normalized critical load vs length to thickness ratio L/h are plotted in Fig. 3 for comparing the results of the elasticity solution with those from other theories. Once again, significant deviation is observed in the case of the CLT, and the higher-order theory agrees very well with the elasticity solution over the complete range of the L/h values.

Next, results are obtained for $[0_5/90_{10}/0_5]$ graphite/epoxy composite laminates and are compared with those obtained using the laminated plate theories described earlier. Comparisons of the transverse shear effect on the normalized critical load, with changes in the magnitude of the delamination length, are presented in Fig. 4 for the relatively thin delamination layer ($h_1/h = 0.9$). Significantly larger deviations are observed not only between the results of the elasticity solution and the CLT; differences are also observed between the results of the elasticity solution and the higher-order theory. This implies that the complexity of transverse shear and transverse normal stress distributions in composites stacked by layers with different angles produces more transverse effects in delamination buckling. It is also seen from the figure that the transverse shear effect becomes smaller as the delamination length increases. This is due to the fact that, with the increase in delamination length, local buckling of the delaminated layer becomes dominant, which causes the local length-to-thickness ratio to be larger. Therefore the transverse shear effect decreases. These phenomena are very similar to those indicated in previous studies by Chattopadhyay and Gu.[9]

The variations of the normalized critical load, with changes in length-to-thickness ratio, are presented in Figs. 5 and 6 for different delamination lengths ($\beta = 0.2$ and 0.5) but fixed delamination location ($h_1/h = 0.9$). As seen from these two figures, at lower values of L/h, large deviations are observed between the elasticity solution and the CLT. The developed higher-order theory shows good agreement with the elasticity solution for thin and moderately thick laminates. However, for thick laminates ($L/h < 10$), even the developed higher-order theory exhibits noticeable deviation from the elasticity solution. For example, at $L/h = 8$, the critical load predicted by the developed higher-order theory is approximately 9 and 3.5% higher than predictions from the elasticity solution for the shorter and longer delaminations, respectively. The shorter the delamination, the larger the transverse shear effect. This phenomenon is very different from what is observed in unidirectional composite plates (see Fig. 2). This is largely due to the complexity of transverse shear and normal stress distributions in cross-ply laminates. Figures 5 and 6 also show that the three solutions converge more rapidly with the increase in the length-to-thickness ratio for longer

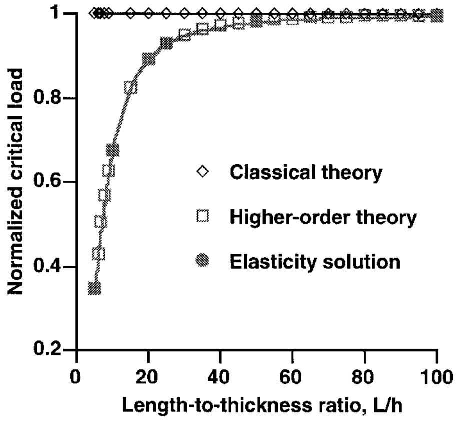

Fig. 3 Comparison of critical load with changes in length-to-thickness ratio (L/h) for unidirectional composites; $h_1/h = 0.9$.

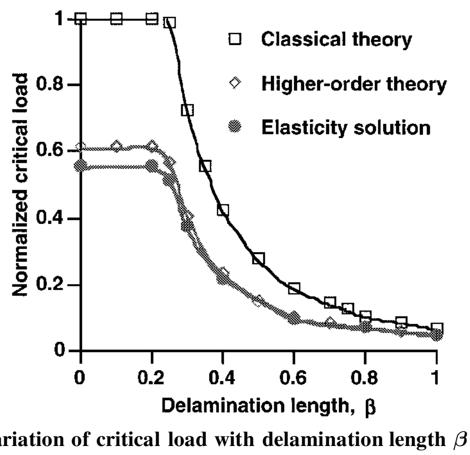

Fig. 4 Variation of critical load with delamination length β for $[0_5/90_{10}/0_5]$ composites; $h_1/h = 0.9$ and $L/h = 10$.

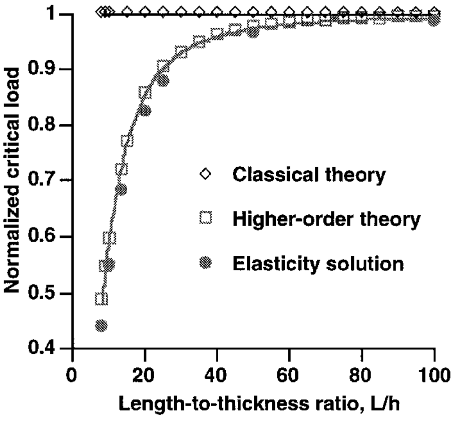

Fig. 5 Variation of critical load with changes in length-to-thickness ratio (L/h) for $[0_5/90_{10}/0_5]$ composites; $h_1/h = 0.9$ and $\beta = 0.2$.

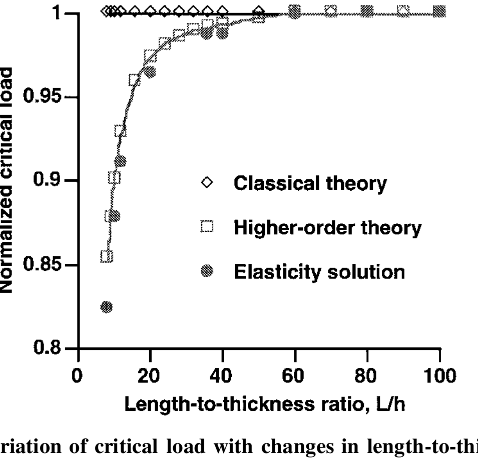

Fig. 6 Variation of critical load with changes in length-to-thickness ratio (L/h) for $[0_5/90_{10}/0_5]$ composites; $h_1/h = 0.9$ and $\beta = 0.5$.

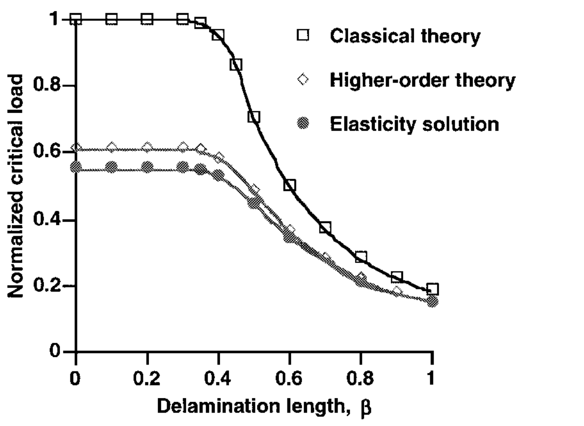

Fig. 7 Variation of critical load with delamination length β for $[0_5/90_{10}/0_5]$ composites; h_1/h = 0.8.

delaminations. The observation agrees with the preceding discussion on the effects of delamination buckling modes.

An example for a thicker delamination ($h_1/h = 0.8$) is also examined. The stacking sequence for the example is $[0_5/90_{10}/0_5]$, and the plate is thick ($L/h = 10$). The variations of the critical loads with delamination length are presented in Fig. 7. Once again, the transverse shear effect becomes smaller as the delamination length increases. However, more deviation is observed for longer delamination ($\beta > 0.35$) in this case, compared with that exhibited by the thinner delamination case (see Fig. 4). The explanation for this phenomenon is a combination of the intrinsic character for the thicker delamination. The first is the slower transition from the global buckling mode to the local delamination buckling mode for the thicker delamination. The second is the increase in the local length-to-thickness ratio for the local delamination buckling mode with the thicker delamination. These two factors eventually increase the transverse effect for the delamination buckling load in the thicker delamination case.

In all examples, results calculated using the previously developed higher-order theory agree very well with those obtained from the present elasticity solution for thin and moderately thick delaminated composite plates. For thick plates, results calculated using the higher-order theory show much smaller deviations than those of the elasticity solution, compared with the classical laminate theory. Because the elasticity solution can be expensive for practical engineering problems (the size of the nonlinear eigenvalue problem in the elasticity solution depends upon the number of layers), the developed higher-order theory is therefore more suitable for delamination buckling analysis of thin and moderately thick composite plates in engineering practice.

IV. Concluding Remarks

In conclusion, an elasticity-theory-based approach has been presented for delamination buckling of composite laminates consisting of arbitrary numbers of orthotropic layers whose behavior is referred to as cylindrical bending. Because the solutions are exact in each defined region within the assumptions of linear elasticity, they are free from the simplifying assumptions imposed by the laminated plate theories. Therefore there are no distinctions between thick and thin plates, and transverse shear deformation and transverse normal deformation are automatically taken into account. The following specific observations have been made.

1) The developed elasticity approach provides the means of assessing the validity of the CLT and other laminated plate theories for the delamination buckling problem. It also provides insight into the basic assumptions required in the formulation of more general theories for composite laminates.

2) The solutions using a developed higher-order theory for the critical load converge to the elasticity solution with much smaller errors (less than 9%) in all examples treated earlier, whereas solutions from CLT show an error of more than 100% for thick laminates. Based on the evidence presented here, the use of the developed higher-order theory in the elastic design, especially for moderately thick and thin laminates, appears adequate.

3) For the delamination problem, the transverse shear effect becomes smaller as the delamination length increases due to the changes in delamination buckling modes.

Acknowledgments

The research was supported by the U.S. Army Research Office, Grant DAAH04-93-G-0043; the Technical Monitor was Gary Anderson.

References

[1] Chai, H., Babcock, C. D., and Krauss, W. G., "One Dimensional Modeling of Failure in Delaminated Laminates," *International Journal of Solids and Structures*, Vol. 17, No. 11, 1981, pp. 1069–1083.

[2] Chai, H., and Babcock, C. D., "Two-Dimensional Modeling of Failure in Laminated Plates by Delamination Buckling," *Journal of Composite Materials*, Vol. 19, No. 1, 1985, pp. 67–98.

[3] Sallam, S., and Simitses, G. J., "Delamination Buckling and Growth of Flat, Cross-Ply Laminates," *Composite Structures*, Vol. 4, No. 3, 1985, pp. 361–381.

[4] Yin, W. L., and Jane, K. C., "Refined Buckling and Postbuckling Analysis of Two-Dimensional Delamination. I: Analysis and Validation," *International Journal of Solids and Structures*, Vol. 29, No. 5, 1992, pp. 591–610.

[5] Yin, W. L., and Jane, K. C., "Refined Buckling and Postbuckling Analysis of Two-Dimensional Delamination. II: Results for Anisotropic Laminates and Conclusion," *International Journal of Solids and Structures*, Vol. 29, No. 5, 1992, pp. 611–639.

[6] Kardomateas, G. A., and Schmueser, D. W., "Buckling and Postbuckling of Delaminated Composites Under Compressive Loads Including Transverse Shear Effects," *AIAA Journal*, Vol. 26, No. 3, 1988, pp. 337–343.

[7] Chen, H. P., "Shear Deformation Theory for Compressive Delamination Buckling and Growth," *AIAA Journal*, Vol. 29, No. 5, 1991, pp. 813–819.

[8] Barbero, E. J., and Reddy, J. N., "Modeling of Delamination in Composite Laminates Using a Layer-Wise Plate Theory," *International Journal of Solids and Structures*, Vol. 28, No. 3, 1991, pp. 373–388.

[9] Chattopadhyay, A., and Gu, H., "A New Higher-Order Plate Theory in Modeling Delamination Buckling of Composite Laminates," *AIAA Journal*, Vol. 32, No. 8, 1994, pp. 1709–1716.

[10] Pagano, N. J., "Exact Solutions for Composite Laminates in Cylindrical Bending," *Journal of Composite Materials*, Vol. 3, No. 3, 1969, pp. 398–411.

[11] Pagano, N. J., "Exact Solutions for Rectangular Bidirectional Composites and Sandwich Plates," *Journal of Composite Materials*, Vol. 4, No. 1, 1970, pp. 20–35.

[12] Pagano, N. J., "Influence of Shear Coupling in Cylindrical Bending of Anisotropic Laminates," *Journal of Composite Materials*, Vol. 4, No. 3, 1970, pp. 330–343.

[13] Pagano, N. J., and Wang, A. S. D., "Further Study of Composite Laminates Under Cylindrical Bending," *Journal of Composite Materials*, Vol. 5, No. 5, 1971, pp. 521–528.

[14] Pagano, N. J., and Hatfield, S. J., "Elastic Behavior of Multilayered Bidirectional Composites," *AIAA Journal*, Vol. 10, No. 5, 1972, pp. 931–933.

[15] Noor, A. K., and Burton, W. S., "Three-Dimensional Solutions for Antisymmetrically Laminated Anisotropic Plates," *Journal of Applied Mechanics*, Vol. 57, No. 1, 1990, pp. 182–188.

[16] Chattopadhyay, A., and Gu, H., "Exact Elasticity Solution for Buckling of Composite Laminates," *Composite Structures*, Vol. 34, No. 2, 1996, pp. 291–299.

G. A. Kardomateas
Associate Editor